

Ionospheric Research

NASA Grant NSG-114-61

Scientific Report

on

Measurement of Electron Content at the Magnetic Equator

by

William J. Ross

March 30, 1966

Scientific Report No.268

Ionosphere Research Laboratory

Submitted by:


W. J. Ross, Professor of Electrical Engineering

Approved by:


**A. H. Waynick, Professor of Electrical
Engineering, Director, Ionosphere Research
Laboratory**

The Pennsylvania State University

College of Engineering

Department of Electrical Engineering

TABLE OF CONTENTS

	Page
Abstract	i
1. Introduction	1
2. Method of Analysis	2
3. Experimental Results	4
a. Solar Variations	4
b. Diurnal Variations	6
c. Seasonal Variations	8
d. Electrodynamic Effects	10
e. Height Variation	10
4. Conclusions	14
Acknowledgements	15
Bibliography	16
Appendix	17

2186

ABSTRACT

Values of the vertical column electron content of the ionosphere at Huancayo, Peru, are presented for an eighteen month interval. These data were obtained from an analysis of Faraday rotation data from a radio beacon satellite. (Transit 4A)

The daytime electron content is found to vary with the 10.7 cm solar radio flux, and after normalization for this dependence the average diurnal variation is found to be quite regular with a range of about 20:1.

A biannual variation in the daytime electron content is found also, with maxima near the equinoxes and with a range of about 2:1.

Reecka

1. Introduction

Over the past few years a great amount of experimental data has been published concerning the variation of electron content at middle latitudes, e.g. Garriott (1960), Ross (1960), and Yeh and Swenson (1961). These studies have been based for the most part on experiments involving radio beacon satellites and on the measurements of the propagation effects in the radio signals from these sources as they pass through the ionosphere. Relatively few data have been published relating to the electron content of the ionosphere at low latitudes, e.g. Somayajulu et.al. (1964). It is the purpose of this study to present the results of a series of measurements made from a station on the magnetic equator, and to discuss the variation of equatorial electron content.

Measurements were made at Huancayo, Peru (1205 S, 75.35 W) from September 1961 to February 1963 of the polarization rotation of the 54 mc/s signals from the satellite 1961 Omicron 1 (Transit 4A). This satellite was launched in a high inclination orbit, approximately circular at about 1000 km altitude, and was magnetically stabilized to a very low residual spin rate. The measurement of electron content therefore refers to the height range up to about 1000 km, and changes in rotation can be attributed entirely to the ionospheric medium. Normally two records were made each day spaced about twelve hours apart at times which precessed earlier each day on the average by about fourteen minutes. In this way measurements were made at all times of day in an elapsed time of about seven weeks, and about eleven such sweeps in local solar time were made during the eighteen month observation period.

2. Method of Analysis

For a station on the magnetic equator the usual polarization rotation ambiguity can be resolved when the satellite source passes in a direction transverse to the magnetic field, for example see Blumle (1962). By counting rotations of the plane of polarization from this transverse point it is therefore possible to determine unambiguously the number of polarization rotations between the satellite and the ground based receiver at any point during the satellite's passage. To a first order approximation the polarization rotation angle Ω is related to the vertical column electron content of the ionosphere below the height of the satellite by the well-known equation

$$\Omega = K \overline{B_L} \sec \chi \int N dh \text{ semi-rotations}$$

where

$$K = 2.582 \cdot 10^{21} \text{ for } 54 \text{ Mc/s,}$$

B_L = the longitudinal component in gammas of the earth's magnetic field along the ray from satellite to receiver,

χ = the zenith angle of the assumed straight line ray path

N = the electron density per cubic meter at height h , and the average bar denotes the weighted mean value of the product over the ray path, which takes this mean value at the "mean ionospheric point".

When ray refraction and other second order effects are included in the analysis, Ross (1965) has shown that the angle of rotation is related to the angle Ω_0 given above by first order theory by the equation

$$\Omega = \Omega_0 [1 + \frac{1}{2} \beta \bar{X} + \frac{1}{2} (\beta - 1) G \bar{X}]$$

where

\bar{X} = the mean square plasma frequency along the ray path normalized to the wave frequency, and which can be determined approximately from the first order equation above,

β = a form factor for the ionization distribution which can be estimated a priori,

and G = a geometric factor relating the relative directions of the ray, the magnetic field and the vertical at the mean ionospheric point.

The inclusion of the second order effects in the analysis resulted in corrections to the first order values of five percent or less, except at the extreme limits of the satellite pass when the zenith angle became large. A further potential source of error at least as great, which could not be corrected for readily, arose from the uncertainty in the height of the mean ionospheric point. This point was taken arbitrarily to be 400 km, a value which is believed to be quite close to the height of the average equatorial ionosphere, as will be discussed later.

The value of B_L was computed from a spherical harmonic expansion of the earth's magnetic field using Jensen-Cain coefficients for epoch 1960. The times of consecutive polarization nulls in the signal amplitude recorded from a linearly polarized antenna were interpolated graphically to give a continuous record of polarization rotation. Values of electron content were then computed for each integral degree latitude crossing of the satellite within the field of

view of the receiving station. Near the center of each record the precision of measurement became relatively poor due to scaling uncertainties in the experimental data. The four values nearest the transverse propagation point were discarded and an average electron content was computed for each satellite pass using the next three values on each side of the transverse point. The estimated absolute accuracy of the results is rather better than ten percent for the daytime records but is perhaps as poor as thirty percent for some nighttime records when the polarization rotation rate was extremely low.

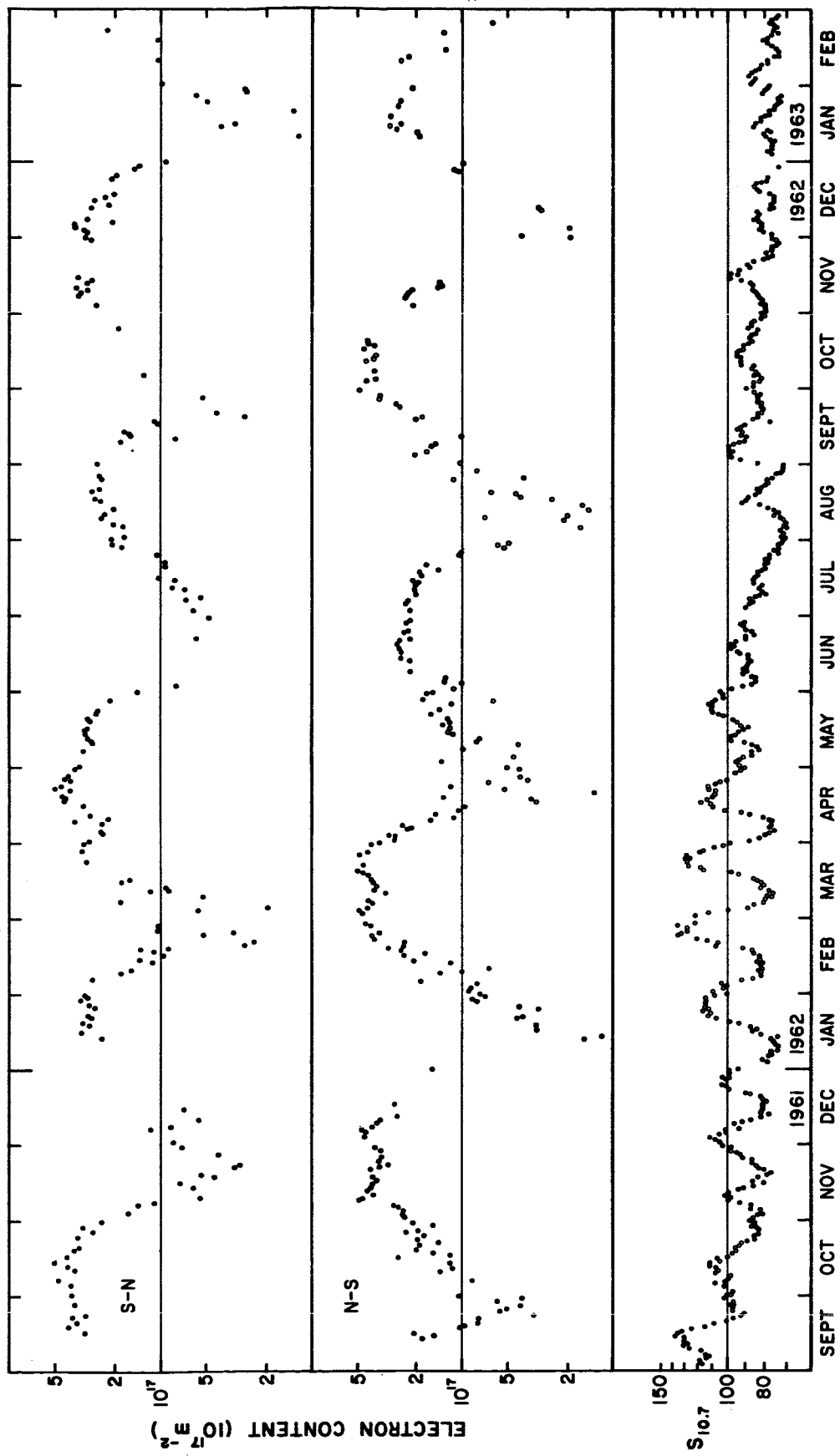
3. Experimental Results

The values of electron content calculated as above are shown in Figure 1. The two sets of data shown are derived respectively for northbound (S-N) and southbound (N-S) satellite passes and in each the diurnal variation, which is produced as the orbit of the satellite precesses in solar time, is clearly evident. For reference the 10.7 cm solar radio flux S is included as an index of solar ultraviolet activity during the same period.

a. Solar Variations

In several of the daytime sequences in Figure 1, in particular for the November 1961 and March 1962 sections of the (N-S) data, an apparent noon decrease in electron content can be seen. This effect is not so pronounced in other daytime sections, in fact quite the contrary appears to be the case in some instances.

A closer investigation of these apparent diurnal variations shows that they correspond in date to the fluctuations in the solar



VARIATION OF ELECTRON CONTENT AT HUANCAYO, PERU

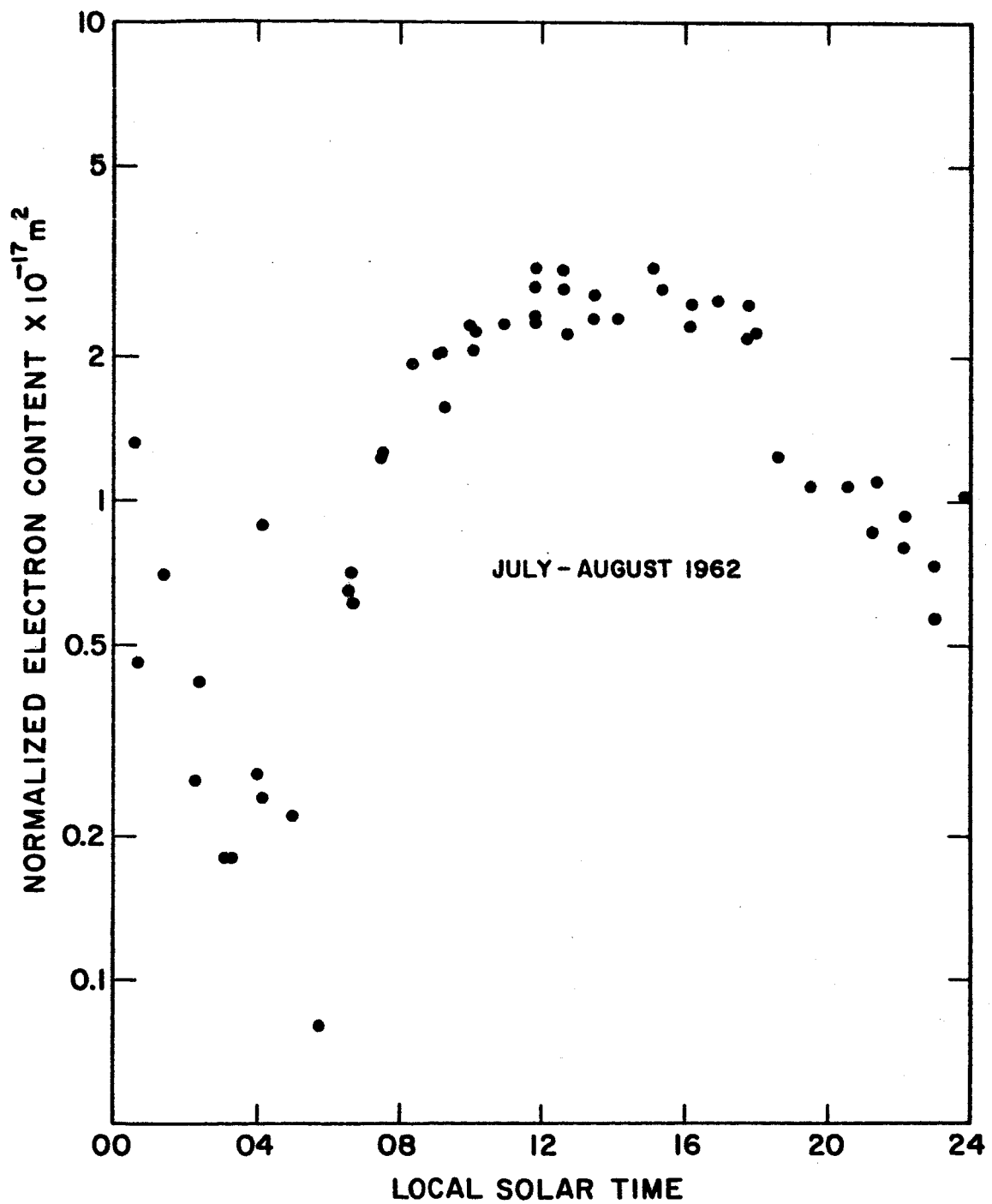
FIGURE 1

radioflux. The electron content was plotted against the solar radioflux value for each series of satellite passes for the four hour interval between 1100 hours and 1500 hours, when the electron content might be supposed to be reasonably constant. Regression lines were drawn through these plots, and where the slope was significant it was found to represent an index of approximately unity. All electron content data were then normalized to a fixed value of solar flux ($S = 100$) assuming this proportionality.

Nicolet (1963) has studied the variation of thermospheric temperature with the solar radioflux S . He found a similar short-term coefficient for effects which could be associated with the solar rotation period of twenty-seven days, but found that for longer periods of the order of months a coefficient of approximately one-half the short period value was relevant. If we assume that both the thermospheric temperature and the electron content of the ionosphere have the same approximately linear relationship to the solar ultraviolet flux, we may consider that a similar short term and long term coefficient relationship will exist for the electron content also. On this basis the monthly levels of electron content were further normalized according to the average solar radioflux for each solar rotation.

b. Diurnal Variations

A representative plot of the variation of electron content with time of day is shown in Figure 2. In this figure the data are taken for a two month period during July and August 1962 and are plotted against the local mean solar time of the ionospheric point for each observation. The principal features in this figure are a well defined broad daytime maximum in electron content falling rather



AVERAGE DIURNAL VARIATION OF
NORMALIZED ELECTRON CONTENT

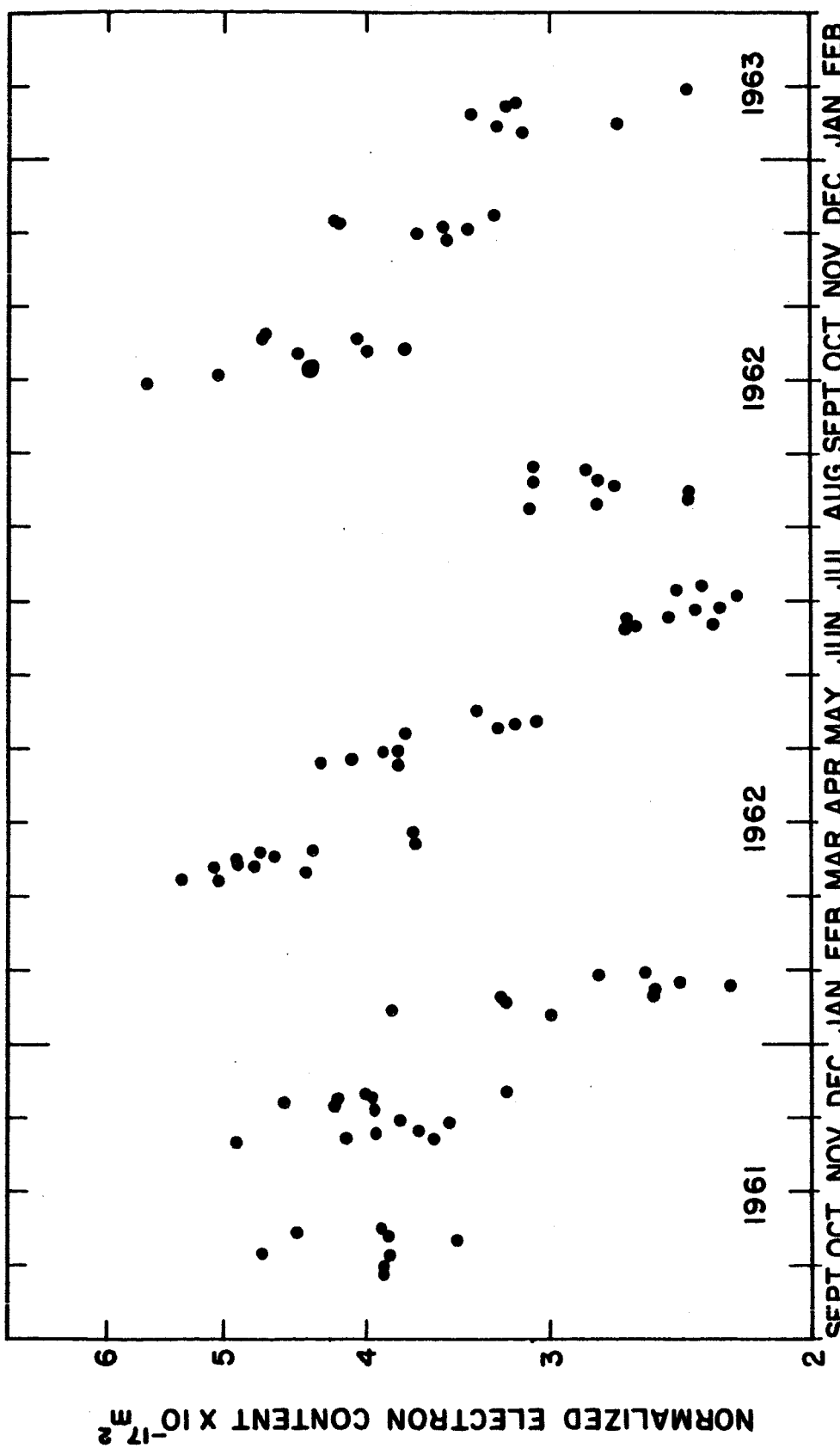
FIGURE 2

irregularly after sunset to a predawn minimum, and then rising rapidly again after sunrise to the daytime maximum value which is reached about three hours after sunrise. The diurnal range of electron content seen in this figure is of the order of twenty to one, but it is likely that this value is somewhat low since in some nighttime records it was impossible to determine a value for electron content because the Faraday rotation rate was so low. This diurnal range of electron content is much greater than that seen at middle latitudes during the same part of the solar cycle, e.g. see Hibberd and Ross (1966), and also is considerably greater than that found by Somayajulu (1964) for a station which is approximately ten degrees off the magnetic equator.

c. Seasonal Variations

It is apparent in Figure 1 that the daytime maximum in electron content ranges over a factor of about two during the course of the year. In order to study this variation further, normalized electron content data have been plotted against date in Figure 3 for local times ranging between 1100 hours and 1600 hours.

In this figure a biannual oscillation in daytime electron content can be seen with maxima occurring near the equinoxes and minima near the solstices. The minimum about the southern winter solstice is much broader than that about the summer solstice. The cosine of the noon solar zenith angle at Huancayo shows a similar biannual variation with maxima and minima at about the same times, but varies only by about twenty percent as compared with the factor of two seen in the normalized electron content data. It does not therefore appear that the zenith angle variation in itself can be



SEASONAL VARIATION OF NORMALIZED DAYTIME ELECTRON CONTENT

FIGURE 3

responsible for most of this effect. In any case the normalization procedures should have removed any simple dependency on solar zenith angle.

d. Electrodynamic Effects

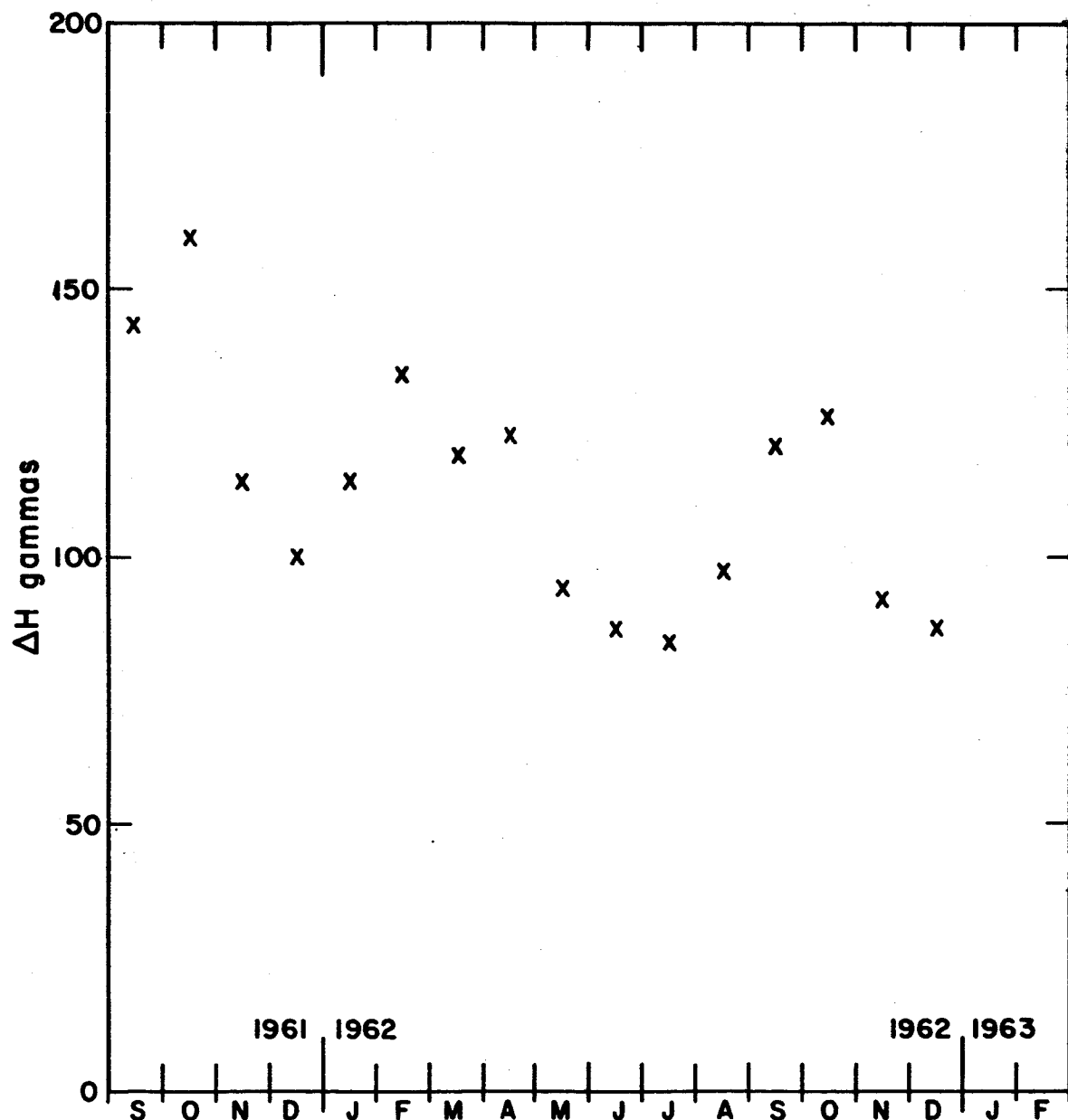
Another property of the equatorial ionosphere which shows a similar biannual variation is the intensity of the equatorial electrojet, for instance, see Vestine et al (1947). The monthly mean of the daily range of horizontal field intensity, ΔH , scaled from Huancayo magnetograms, is shown in Figure 4. The equinoctial maxima are clearly evident and the annual range is about fifty percent.

Attempts to find a corresponding relationship between the day to day variations in electron content and in diurnal magnetic field strength variation were unsuccessful. In fact, in some cases, it seemed that a barely significant negative correlation obtained.

A number of theories of the equatorial F region, e. g. Martyn (1959), propose vertically directed motor forces arising from the electric fields due to the flow of the Sq current system in the E region of the ionosphere. It is possible that some of the biannual variations seen in the electron content data in this paper arise from this cause, but the lack of detailed correlation prevents any positive identification of this effect at this time.

e. Height Variation

Electron density profiles of the bottomside of the ionosphere over Huancayo were available for several months of the observation period. Taken in conjunction with the electron content data, these



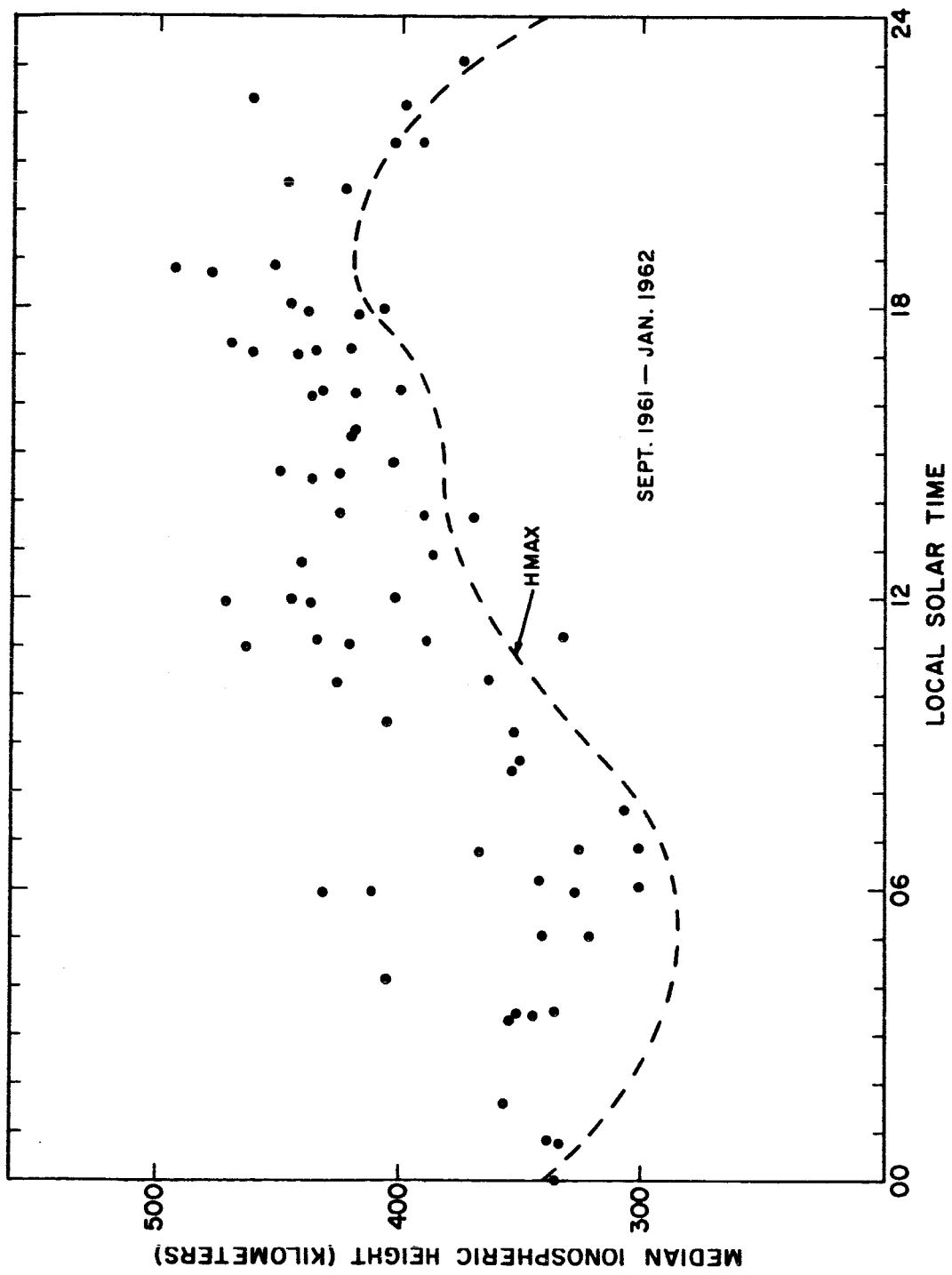
MONTHLY MEAN DAILY VARIATION OF H

FIGURE 4

profiles enabled an improved determination to be made of the height distribution of ionization throughout the equatorial F region.

By extrapolating the bottomside profiles beyond the nose of the F region it was possible to determine the median height of the ionization. The results are quite insensitive to the particular extrapolation method used, and are shown in Figure 5. The diurnal trend is clearly evident with the median height rising from its nighttime value of approximately 340 km to daytime values about 420 km, and falling again to the nighttime value several hours after sunset. The unusually large values seen around sunrise are considered to be inaccurate due to the rapidly changing nature of the ionosphere at that time.

Since for an equatorial station the value of $B_L \sec \chi$ has a fairly uniform logarithmic gradient with height of approximately 10^{-3} km^{-1} , the mean ionospheric height used in Faraday rotation calculations is approximately at the centroid of the ionization distribution. Because of the skewness of the height distribution, this centroid should lie somewhat above the median height, perhaps by 30 km or so. The constant height value of 400 km which has been assumed in the analysis of electron content data therefore, is approximately correct, and the principal effect of the diurnal height variation of the ionosphere will be to compress by about ten percent the apparent diurnal range of electron content variation.



AVERAGE DIURNAL VARIATION OF IONOSPHERIC HEIGHT
FIGURE 5

4. Conclusions

Polarization rotation measurements from an equatorial station of beacon satellite radio transmissions enable the vertical column electron content of the equatorial ionosphere to be measured to an accuracy of better than ten percent. Measurements made over an extended period of time can be used to study diurnal, "seasonal", and other effects.

Some day to day variations in electron content were found to be closely correlated with the solar radioflux at 10 cm, confirming similar correlations of thermospheric temperature etc, made by other workers. When this kind of solar variability was allowed for, the average diurnal variation pattern became quite smoothly varying with a range of greater than 20:1.

A pronounced "seasonal" variation in electron content was found to be similar in form to the variation in the strength of the equatorial electrojet. However a similar result could not be found for day to day variations and a positive identification of the effects of electrodynamic drift forces in the equatorial ionosphere cannot be made at this time.

Comparison of the electron content data with reduced vertical sounding ionograms showed that the mean ionospheric height has a pronounced diurnal variation quite similar in form to the variation of the height of the F layer maximum.

Acknowledgments

The cooperation of the Instituto Geofisico del Peru in operating the recording station at Huancayo, and in scaling critical frequencies from concurrent ionograms is gratefully acknowledged. Reduced electron density profiles used in the analyses were provided by the Central Radio Propagation Laboratory, Boulder. Orbital data were supplied by the Applied Physics Laboratory, John Hopkins University. Magnetic field computations were made by the Planetary Atmospheres Division of the Goddard Space Flight Center.

This work was supported by the National Aeronautics and Space Administration under grant NsG 114-61.

Bibliography

- Blumle, L. J., "Satellite Observations of the Equatorial Ionosphere" J. Geophys. Res., 67, p. 4601, (1962).
- Garriott, O. K., "The Determination of Ionospheric Electron Content and Distribution from Satellite Observations" J. Geophys. Res., 65, p. 1139, (1960).
- Hibberd, F. H. and W. J. Ross, "The Total Electron Content of the Ionosphere in Middle Latitudes" J. Geophys. Res., 71, (1966) (in press)
- Martyn, D. F., "The Normal F Region of the Ionosphere" Proc. I.R.E. 47, p. 147, (1959).
- Nicolet, M., "Solar Radio Flux and Temperature of the Upper Atmosphere" J. Geophys. Res., 68, p. 6121, (1963).
- Ross, W. J., "The Determination of Ionospheric Electron Content from Satellite Doppler Measurements" J. Geophys. Res., 65, p. 2601, (1960).
- Ross, W. J., "Second-Order Effects in High-Frequency Transionospheric Propagation" J. Geophys. Res., 70, p. 597, (1965).
- Somayajulu, Y. V., T. R. Tyagi, and V. P. Bhatnagar "Ionospheric Electron Content and its Variations from Faraday Fading of Satellite Radio Transmissions" Space Research IV, p. 498, (1964).
- Vestine, E. H., L. Laporte, I. Lange and W. E. Scott "The Geomagnetic Field, Its Description and Analysis" Carnegie Institute of Washington Publication 580 (1947).
- Yeh, K. C. and G. W. Swenson, "Ionospheric Electron Content and its Variations deduced from Satellite Observations" J. Geophys. Res., 66, p. 1061, (1961).

APPENDIX

This appendix contains separate tabulations of experimental data in chronological order for each direction of satellite passage. The column headings are as follows.

DATE = a six-digit designation in the form year-month-day.

TIME = time of transverse propagation, 75W Standard Time.

HEIGHT = satellite height in kilometers.

N MAX = F-layer peak density at the time of satellite passage
read from Huancayo ionograms, in units of 10^{12} m^{-3}

S₁₀ = average 10.7 cm radio flux for DATE in units of 10^{-22}
 $\text{W m}^{-2} \text{ sec.}$

N_T = vertical column electron content in units of 10^{17} m^{-2}
calculated as indicated in Section 2

N_T* = normalized vertical column electron content in units
of 10^{17} m^{-2} calculated as indicated in Section 3.

Appendix A

Northbound Satellite Passes

<u>Date</u>	<u>Time</u>	<u>Height</u>	<u>N Max</u>	<u>S₁₀</u>	<u>N_T</u>	<u>N_T[*]</u>
610915	1804	956	1.00	135	3.20	2.48
610917	1703	956	0.98	124	4.04	3.42
610919	1714	958	0.80	108	3.52	3.39
610921	1613	959	1.11	96	3.86	4.18
610922	1618	960	0.93	92	3.17	3.58
610926	1528	964	1.04	98	3.69	3.87
610930	1436	966	0.83	100	3.80	3.88
611004	1346	968	0.98	102	3.88	3.84
611006	1245	968	1.08	101	4.70	4.70
611010	1155	971	0.69	106	3.68	3.47
611011	1200	973	0.90	107	4.12	3.85
611013	1100	973	1.03	111	4.96	4.46
611015	1110	974	0.96	106	4.17	3.90
611018	1014	976	0.88	95	3.74	3.90
611019	1020	977	1.57	95	3.50	3.64
611023	0928	979	0.96	85	3.50	4.03
611025	0827	980	1.19	83	2.78	3.28
611027	0838	981	1.47	84	3.22	3.72
611029	0737	981	1.35	85	2.45	2.76
611103	0652	984	0.94	81	1.65	1.96
611106	0556	986	0.75	87	1.41	1.54
611107	0602	987	0.59	93	1.10	1.13
611109	0501	987	0.26	98	0.56	0.54
611113	0410	988	0.24	91	0.61	0.64
611115	0420	989	---	80	0.77	0.91
611117	0320	990	---	83	0.45	0.51
611118	0324	991	0.30	79	0.54	0.52
611121	0229	991	---	83	0.33	0.38
611122	0234	992	0.20	84	0.30	0.34
611126	0143	993	---	93	0.42	0.42
611129	0048	994	---	98	0.72	0.70
611201	2352	995	---	105	0.83	0.75
611206	2306	997	0.69	101	1.17	1.11
611207	2311	996	---	94	0.87	0.89
611210	2216	997	0.42	87	0.56	0.62
611214	2125	998	0.45	81	0.70	0.84
620112	1425	999	0.64	77	2.45	2.99
620114	1435	998	0.94	82	3.34	3.83
620117	1339	997	0.88	87	2.97	3.21
620118	1345	998	0.86	94	3.23	3.23
620120	1244	998	0.63	107	2.87	2.55
620121	1249	997	1.09	112	3.00	2.55
620124	1153	997	0.61	114	2.71	2.26
620125	1158	997	1.09	115	2.94	2.45
620127	1058	997	1.22	115	3.39	2.83
620128	1103	996	1.04	115	3.08	2.59
620129	1108	996	1.20	109	3.13	2.79

<u>Date</u>	<u>Time</u>	<u>Height</u>	<u>N Max</u>	<u>S₁₀</u>	<u>N_T</u>	<u>N_T[*]</u>
620205	0921	993	0.82	92	2.80	2.99
620208	0826	994	0.86	82	1.84	2.20
620209	0831	992	0.80	83	1.57	1.86
620212	0735	991	0.59	81	1.13	1.38
620213	0739	989	0.74	84	1.39	1.64
620215	0640	990	0.47	83	0.97	1.16
620216	0644	990	0.52	86	1.11	1.28
620217	0659	988	0.82	87	1.37	1.56
620219	0549	988	0.10	108	0.29	0.26
620220	0554	986	0.12	107	0.24	0.22
620223	0458	986	0.22	136	0.53	0.38
620224	0503	984	0.18	134	0.33	0.25
620225	0508	983	0.56	129	1.06	0.82
620227	0407	983	0.45	136	1.06	0.78
620303	0317	980	---	100	0.57	0.57
620304	0322	978	0.08	89	0.20	0.22
620306	0221	978	---	81	1.85	2.23
620308	0232	975	0.37	77	0.54	0.70
620310	0132	975	---	76	1.18	1.55
620311	0136	975	0.57	78	0.89	1.14
620312	0141	972	0.53	82	0.93	1.13
620314	0040	971	---	82	1.83	2.24
620315	0045	969	1.09	84	1.60	1.90
620321	2257	965	1.24	128	3.08	2.40
620325	2208	962	1.27	118	3.29	2.79
620328	2112	958	---	103	3.20	3.11
620329	2117	955	0.98	99	2.70	2.72
620330	2123	958	---	92	2.82	3.06
620402	2027	956	---	80	2.41	3.01
620403	2032	955	1.04	78	2.50	3.20
620406	1936	952	1.27	77	2.43	3.15
620407	1941	951	1.47	77	3.61	4.69
620409	1840	952	0.78	78	2.22	2.85
620410	1845	949	1.14	81	2.91	3.60
620414	1755	945	1.07	110	3.27	2.97
620416	1654	946	1.57	119	4.31	3.62
620417	1700	945	1.37	114	4.29	3.76
620418	1704	943	1.60	110	4.49	4.08
620420	1603	942	1.24	109	3.98	3.65
620421	1608	941	1.65	112	4.98	4.45
620422	1613	940	1.39	113	4.56	4.03
620424	1512	939	1.07	105	3.98	3.79
620425	1519	937	1.42	101	4.34	4.30
620426	1523	936	1.29	100	4.08	4.08
620429	1428	934	1.07	93	3.62	3.89
620430	1432	933	---	91	3.45	3.79
620506	1241	930	0.80	87	3.26	3.75
620509	1145	928	0.66	87	2.83	3.25
620510	1150	926	0.78	91	2.88	3.16
620511	1155	925	0.74	98	3.01	3.07
620513	1055	926	1.19	96	3.18	3.31

<u>Date</u>	<u>Time</u>	<u>Height</u>	<u>N MAX</u>	<u>S₁₀</u>	<u>N_T</u>	<u>N_T</u> [*]
620514	1059	923	0.84	94	3.22	3.42
620515	1104	922	0.92	91	3.05	3.36
620518	1009	920	0.76	95	2.94	3.06
620519	1012	920	0.68	97	3.07	3.13
620521	0913	920	0.96	106	2.64	2.46
620522	0919	918	1.02	110	2.63	2.37
620526	0828	916	0.78	110	2.19	1.97
620530	0737	912	---	105	1.45	1.36
620602	0641	910	---	92	0.80	0.86
620621	0223	899	0.24	90	0.59	0.62
620629	0041	895	0.24	(90)	0.48	(0.50)
620701	2346	894	0.32	(90)	0.62	(0.65)
620705	2255	892	0.38	86	0.69	0.74
620706	2300	890	---	88	0.55	0.57
620709	2203	890	---	81	0.71	0.80
620710	2209	889	---	83	0.86	0.94
620713	2113	887	---	86	0.81	0.86
620714	2118	887	---	85	1.03	1.10
620718	2029	885	0.53	80	0.95	1.08
620720	1927	885	---	79	0.94	1.08
620724	1837	883	0.44	78	1.08	1.25
620727	1741	882	0.57	74	1.81	2.20
620728	1746	882	0.90	74	2.12	2.58
620731	1650	881	0.57	73	2.14	2.64
620801	1656	880	0.57	71	1.78	2.25
620805	1605	879	0.70	70	1.80	2.31
620806	1609	878	0.63	72	2.08	2.59
620808	1509	879	---	72	2.50	3.09
620810	1519	877	0.93	76	2.38	2.78
620812	1406	878	0.53	76	2.07	2.42
620815	1323	876	0.68	92	2.47	2.42
620816	1328	877	0.64	90	2.72	2.72
620819	1232	876	0.63	83	2.84	3.08
620820	1236	876	0.88	84	2.57	2.79
620824	1146	874	0.61	79	2.46	2.83
620825	1151	874	0.68	77	2.58	3.08
620831	0945	874	0.70	75	2.65	3.28
620909	0824	873	0.86	94	1.86	1.86
620911	0723	873	0.70	90	1.60	1.67
620912	0728	872	0.80	93	1.63	1.64
620913	0733	872	0.76	92	1.77	1.81
620916	0637	872	0.53	91	1.04	1.07
620917	0642	872	0.53	78	1.11	1.34
620919	0541	872	0.09	84	0.29	0.32
620920	0546	872	0.22	84	0.44	0.49
620926	0355	874	---	84	0.54	0.60
621005	0215	875	0.64	86	1.30	1.42
621103	1925	883	0.96	80	2.69	3.13
621107	1834	884	1.39	84	3.49	3.82
621108	1836	885	1.55	85	3.40	3.68
621109	1837	886	0.78	86	3.04	3.25
621110	1742	886	1.58	(87)	3.59	(3.79)

<u>Date</u>	<u>Time</u>	<u>Height</u>	<u>N MAX</u>	<u>S₁₀</u>	<u>N_T</u>	<u>N_T*</u>
621112	1744	888	1.50	88	3.08	3.22
621113	1745	889	1.58	93	2.87	2.84
621114	1650	888	1.83	99	3.50	3.25
621129	1324	897	1.04	75	2.90	3.52
621130	1325	898	0.86	77	3.13	3.70
621202	1326	901	0.84	81	3.03	3.41
621203	1233	900	1.02	83	3.24	3.55
621204	1233	900	1.16	82	3.76	4.17
621205	1234	903	1.09	82	3.79	4.21
621207	1141	903	0.80	86	3.08	3.26
621212	1050	907	1.24	76	2.90	3.48
621213	1052	908	1.07	77	2.21	2.61
621215	0957	908	1.16	76	2.76	3.30
621216	0959	910	---	76	2.36	2.79
621217	1000	911	0.98	78	2.30	2.66
621223	0815	913	0.90	79	2.10	2.39
621225	0817	917	0.70	(75)	1.99	(2.35)
621227	0724	917	0.59	(75)	1.50	(1.77)
621228	0725	918	0.64	74	1.42	1.72
621230	0631	918	0.46	(75)	0.94	(1.11)
630110	0357	925	---	80	0.12	0.14
630112	0358	928	---	78	0.08	0.10
630114	0305	928	0.22	86	0.41	0.42
630115	0306	929	---	85	0.33	0.34
630120	0215	933	---	78	0.13	0.15
630124	0124	935	---	73	0.49	0.60
630126	0030	936	---	73	0.59	0.71
630128	0033	937	0.17	80	0.27	0.30
630129	2338	937	---	79	0.28	0.32
630201	2246	937	0.37	87	0.99	1.01
630210	2105	939	---	79	1.04	1.17
630218	1922	952	0.80	81	1.06	1.16
630222	1831	955	0.94	76	2.26	2.67

Appendix B

Southbound Satellite Passes

<u>Date</u>	<u>Time</u>	<u>Height</u>	<u>N MAX</u>	<u>S₁₀</u>	<u>N_{T-}</u>	<u>N_{T-}</u> [*]
610913	0646	902	0.63	130	1.81	1.48
610914	0650	901	0.62	137	1.51	1.16
610915	0655	901	---	135	2.06	1.60
610917	0555	899	0.23	124	1.03	0.87
610918	0600	899	0.24	115	0.96	0.88
610919	0604	900	0.40	108	0.78	0.75
610921	0504	898	0.43	96	0.78	0.85
610922	0509	897	0.17	92	0.34	0.38
610924	0410	896	0.19	97	0.57	0.61
610925	0413	896	0.37	97	0.51	0.55
610926	0418	895	0.25	98	0.42	0.44
610928	0319	894	0.30	96	0.58	0.62
610929	0323	894	0.25	102	0.40	0.41
610930	0327	895	0.62	100	1.05	1.07
611006	0137	891	0.38	101	0.87	0.86
611010	0047	890	0.62	106	1.39	1.30
611011	0050	890	0.47	107	1.16	1.07
611013	2356	889	0.57	111	1.20	1.07
611015	0001	888	1.30	106	2.67	2.47
611016	2300	887	---	100	1.20	1.18
611017	2304	888	---	97	1.55	1.56
611018	2309	887	---	95	2.00	2.06
611020	2210	888	1.00	93	2.90	3.02
611021	2215	887	---	92	1.43	1.50
611022	2219	886	---	89	2.00	2.18
611024	2119	886	---	85	1.78	2.04
611025	2124	885	1.18	83	2.37	2.77
611026	2127	885	0.96	83	1.98	2.31
611028	2028	884	0.43	86	1.58	1.76
611029	2033	885	0.80	85	2.12	2.39
611101	1938	884	---	86	2.40	2.68
611102	1943	883	0.84	83	2.48	2.86
611104	1842	883	1.04	82	2.46	2.88
611105	1847	883	0.76	87	2.67	2.91
611106	1852	883	1.63	87	2.90	3.17
611108	1751	883	2.31	99	4.92	4.72
611109	1756	883	1.52	98	4.68	4.53
611110	1800	883	1.71	101	4.04	3.80
611112	1701	883	1.30	94	4.38	4.43
611113	1706	883	1.16	91	4.16	4.34
611114	1709	882	1.18	86	4.04	4.46
611116	1610	882	0.97	86	3.79	4.18
611117	1615	881	1.25	83	4.10	4.64
611120	1519	882	1.21	80	4.17	4.90
611121	1524	882	1.00	83	3.60	4.12
611122	1449	881	0.82	84	3.18	3.59
611124	1428	882	0.91	87	3.61	3.94

<u>Date</u>	<u>Time</u>	<u>Height</u>	<u>N MAX</u>	<u>S₁₀</u>	<u>N_T</u>	<u>N_T[*]</u>
611125	1434	881	0.92	92	3.56	3.68
611128	1338	882	1.69	98	3.61	3.50
611129	1343	882	1.50	98	3.91	3.79
611203	1253	882	1.95	111	4.60	3.95
611205	1153	882	1.13	101	4.43	4.21
611206	1156	883	---	101	4.78	4.55
611207	1201	883	1.20	94	4.10	4.18
611209	1102	884	1.08	92	3.79	3.96
611210	1106	883	1.38	87	3.64	4.01
611211	1111	882	1.25	82	2.74	3.20
611216	0916	884	1.17	81	2.86	3.38
611230	0652	886	0.80	94	1.58	1.58
620112	0316	892	---	77	0.16	0.19
620113	0320	891	---	74	0.12	0.15
620116	0225	893	---	84	0.32	0.36
620117	0229	893	0.18	87	0.33	0.36
620120	0135	895	0.31	107	0.44	0.39
620121	0139	894	0.23	112	0.40	0.34
620124	0043	896	---	114	0.31	0.27
620125	0048	897	---	115	0.42	0.36
620126	2348	898	---	115	0.81	0.68
620127	2353	898	---	115	0.87	0.73
620128	2358	898	---	109	0.71	0.63
620130	2258	900	---	102	0.74	0.70
620131	2303	900	---	110	0.91	0.80
620201	2307	900	---	103	0.88	0.84
620203	2207	903	---	104	0.80	0.75
620204	2212	902	0.96	92	1.89	2.02
620207	2116	905	0.88	82	1.40	1.67
620208	2120	905	0.68	83	1.01	1.19
620209	2125	904	0.64	81	0.67	0.82
620211	2025	908	0.72	81	1.20	1.46
620212	2030	907	0.96	84	2.09	2.46
620214	1930	910	0.96	83	2.42	2.89
620215	1935	909	0.88	86	1.76	2.02
620216	1939	910	1.04	87	2.59	2.94
620218	1839	911	1.63	91	3.17	3.45
620219	1844	912	1.32	108	2.46	2.26
620220	1848	913	1.14	107	2.43	2.25
620222	1749	915	1.42	121	3.94	3.26
620223	1754	915	1.77	136	4.09	3.01
620224	1758	916	1.02	134	3.70	2.76
620227	1703	918	1.00	136	4.19	3.08
620228	1707	917	1.16	122	4.49	3.68
620302	1607	921	1.14	112	4.76	4.25
620303	1612	920	1.53	100	4.96	4.96
620304	1616	921	1.50	89	4.38	4.92
620306	1517	923	0.96	81	4.08	5.03
620307	1521	924	1.33	80	4.30	5.37
620310	1426	926	0.80	76	3.34	4.39
620311	1430	927	1.09	78	3.93	5.04
620313	1330	930	1.09	81	3.87	4.77

<u>Date</u>	<u>Time</u>	<u>Height</u>	<u>N MAX</u>	<u>S₁₀</u>	<u>N_T</u>	<u>N_T[*]</u>
620314	1335	930	1.11	82	4.00	4.88
620315	1339	930	1.14	84	4.11	4.90
620317	1239	933	1.22	94	4.34	4.61
620318	1245	933	1.34	98	4.60	4.70
620319	1249	933	1.62	116	5.04	4.35
620321	1149	936	1.07	127	4.68	3.69
620325	1058	939	1.58	128	4.91	3.84
620326	1103	940	1.53	118	4.38	3.71
620329	1007	942	1.65	103	4.10	3.98
620330	1011	943	1.42	99	3.65	3.69
620401	0912	945	0.92	88	2.89	3.28
620402	0917	945	0.92	83	2.87	3.45
620403	0921	946	1.16	80	3.16	3.95
620405	0823	949	0.96	76	2.32	3.05
620406	0827	948	1.29	78	2.19	2.81
620407	0830	949	1.16	77	2.50	3.25
620409	0731	951	0.88	78	1.64	2.11
620410	0736	951	0.76	81	1.14	1.40
620411	0746	950	1.09	88	1.50	1.70
620413	0640	954	0.61	102	1.08	1.06
620414	0645	954	0.57	110	0.95	0.87
620416	0544	956	0.08	119	0.33	0.28
620417	0550	957	0.13	114	0.35	0.31
620418	0554	957	---	110	1.32	1.20
620420	0454	959	0.07	109	0.14	0.13
620421	0459	959	0.25	112	0.53	0.48
620422	0503	960	0.35	113	1.19	1.06
620424	0403	963	0.29	105	0.68	0.65
620425	0408	962	---	101	0.37	0.37
620426	0412	963	0.19	100	0.42	0.42
620429	0317	965	0.25	93	0.42	0.46
620430	0321	964	0.40	91	0.51	0.56
620502	0222	968	0.64	95	1.38	1.46
620504	0231	967	0.23	91	0.46	0.51
620507	0136	971	0.49	83	0.98	1.18
620509	0035	973	0.25	87	0.43	0.49
620510	0040	973	0.31	91	0.80	0.88
620511	0044	973	0.36	98	0.79	0.81
620512	2346	975	0.47	96	1.14	1.19
620513	2350	975	0.52	94	1.22	1.30
620514	2354	975	0.47	91	1.21	1.33
620516	2254	978	0.53	93	1.36	1.45
620517	2259	977	0.41	95	1.21	1.26
620518	2303	978	---	97	1.27	1.29
620520	2204	980	---	106	1.61	1.50
620522	2212	979	0.55	111	1.44	1.29
620524	2113	982	0.64	112	1.18	1.04
620525	2119	982	---	110	0.64	0.57
620526	2122	981	1.02	109	1.82	1.65
620528	2023	984	0.63	104	1.72	1.64
620529	2026	984	---	105	1.58	1.49

<u>Date</u>	<u>Time</u>	<u>Height</u>	<u>N MAX</u>	<u>S₁₀</u>	<u>N_{T-}</u>	<u>N_{T-}</u> [*]
620531	1927	986	0.59	104	1.48	1.41
620601	1932	986	---	98	1.15	1.16
620602	1938	986	---	87	1.01	1.15
620604	1836	988	---	85	1.30	1.52
620605	1841	988	---	85	1.30	1.51
620608	1745	990	0.92	90	2.24	2.46
620612	1655	992	0.55	88	2.27	2.52
620613	1700	991	0.88	89	2.59	2.82
620616	1604	993	0.64	95	2.57	2.60
620617	1608	992	0.66	98	2.68	2.63
620619	1508	994	0.63	98	2.75	2.66
620620	1513	995	0.76	96	2.66	2.63
620621	1517	995	0.55	90	2.23	2.32
620623	1418	996	0.57	86	2.44	2.66
620624	1423	995	0.57	87	2.31	2.49
620627	1327	997	0.63	93	2.38	2.38
620628	1332	997	0.59	91	2.25	2.30
620702	1242	998	0.53	93	2.24	2.24
620705	1146	1000	0.80	88	2.36	2.47
620706	1150	999	0.61	86	2.22	2.37
620709	1055	1000	0.50	80	2.06	2.38
620710	1059	1000	0.61	81	2.10	2.39
620712	1000	1002	0.61	82	2.08	2.33
620713	1005	1001	0.78	86	1.98	2.09
620714	1008	1002	0.74	86	2.16	2.29
620716	0909	1002	0.47	84	1.88	2.04
620717	0914	1001	0.47	84	1.90	2.05
620718	0919	1002	0.50	82	1.43	1.59
620720	0818	1003	0.61	80	1.71	1.95
620724	0727	1003	---	78	1.06	1.22
620725	0734	1003	0.52	74	1.04	1.26
620727	0633	1003	0.14	74	0.53	0.65
620728	0637	1003	---	74	0.59	0.71
620729	0642	1003	0.21	73	0.50	0.61
620801	0546	1003	---	71	0.06	0.08
620805	0457	1003	---	70	0.17	0.22
620808	0400	1003	0.11	72	0.22	0.27
620809	0405	1003	---	73	0.72	0.89
620810	0408	1003	---	76	0.20	0.24
620812	0309	1003	0.03	76	0.15	0.18
620814	0318	1003	0.15	83	0.17	0.18
620816	0219	1002	0.10	90	0.26	0.26
620817	0223	1003	0.24	89	0.41	0.42
620819	0123	1002	0.32	84	0.65	0.70
620824	0037	1002	0.63	79	1.14	1.32
620825	0041	1002	---	77	0.39	0.46
620827	2347	1000	---	72	0.80	1.03
620831	2256	999	---	84	1.04	1.15
620903	2200	998	0.92	99	2.09	1.98
620904	2205	998	0.86	98	1.73	1.66
620906	2105	997	0.68	100	1.60	1.50
620907	2110	998	0.57	97	1.52	1.47

<u>Date</u>	<u>Time</u>	<u>Height</u>	<u>N MAX</u>	<u>S₁₀</u>	<u>N T-</u>	<u>N T-</u> [*]
620910	2014	996	---	90	1.02	1.06
620915	1928	995	0.64	93	1.50	1.52
620918	1833	994	0.74	86	2.04	2.23
620919	1838	993	0.80	84	1.86	2.08
620923	1746	992	0.72	82	2.65	3.04
620924	1751	993	1.00	82	2.80	3.21
620926	1651	990	1.29	84	3.70	4.14
620927	1655	990	1.27	84	3.64	4.07
620929	1556	989	1.37	83	4.98	5.64
620930	1601	989	1.37	90	4.69	4.90
621003	1505	988	1.32	83	4.45	5.04
621004	1510	988	0.96	82	3.83	4.39
621007	1415	986	0.94	85	3.93	4.35
621011	1324	983	1.14	93	4.45	4.45
621012	1328	983	1.00	93	3.99	3.99
621013	1332	984	0.92	95	3.82	3.74
621016	1237	981	1.04	91	4.60	4.70
621017	1242	982	0.96	91	3.97	4.06
621018	1138	980	0.88	89	4.22	4.41
621019	1142	980	---	87	4.38	4.69
621103	0816	970	1.19	80	2.11	2.45
621106	0721	969	0.98	83	2.39	2.64
621107	0724	968	1.19	84	2.32	2.54
621108	0725	968	1.09	85	2.27	2.46
621109	0724	968	1.00	86	2.16	2.31
621110	0633	966	0.59	(86)	1.45	(1.55)
621111	0633	966	0.61	87	1.37	1.45
621112	0634	965	0.59	88	1.42	1.48
621130	0217	953	---	77	0.19	0.23
621201	0216	952	---	77	0.41	0.48
621205	0124	948	---	82	0.20	0.22
621211	2341	944	0.38	78	0.30	0.35
621212	2341	943	0.37	76	0.32	0.38
621226	2014	933	0.70	(75)	1.07	(1.25)
621227	2015	932	0.90	(75)	1.12	(1.32)
621229	1922	930	0.49	(75)	0.98	(1.15)
630110	1647	922	1.09	80	1.92	2.14
630111	1648	922	1.11	81	1.96	2.15
630113	1555	920	0.82	79	2.77	3.12
630114	1555	920	1.19	86	3.14	3.25
630115	1556	918	0.66	85	2.57	2.69
630118	1504	917	---	80	3.05	3.39
630122	1413	915	0.78	75	2.70	3.21
630124	1319	914	1.14	73	2.60	3.17
630129	1229	909	0.50	79	2.15	2.42
630210	0955	904	0.90	79	2.55	2.87
630211	0955	903	0.84	76	2.28	2.67
630214	0904	902	0.68	75	1.29	1.53
630221	0720	899	0.76	74	1.32	1.59
630225	0627	897	0.32	78	0.64	0.74